

Article

Evaluation of Candidate Reference Genes for Gene Expression Analysis in Wild *Lamiophlomis rotata*

Luhao Wang ¹, Feng Qiao ^{1,2,3,*}, Guigong Geng ⁴ and Yueheng Lu ¹

¹ School of Life Sciences, Qinghai Normal University, Xining 810008, China

² Academy of Plateau Science and Sustainability, Qinghai Normal University, Xining 810008, China

³ Key Laboratory of Tibetan Plateau Medicinal Plant and Animal Resources, Qinghai Normal University, Xining 810008, China

⁴ Academy of Agricultural and Forestry Sciences, Qinghai University, Xining 810016, China

* Correspondence: qiaofnm@163.com; Tel.: +86-13619716463

Abstract: *Lamiophlomis rotata* (Benth.) Kudo is a perennial and unique medicinal plant of the Qinghai–Tibet Plateau. It has the effects of diminishing inflammation, activating blood circulation, removing blood stasis, reducing swelling, and relieving pain. However, thus far, reliable reference gene identifications have not been reported in wild *L. rotata*. In this study, we identified suitable reference genes for the analysis of gene expression related to the medicinal compound synthesis in wild *L. rotata* subjected to five different-altitude habitats. Based on the RNA-Seq data of wild *L. rotata* from five different regions, the stability of 15 candidate internal reference genes was analyzed using geNorm, NormFinder, BestKeeper, and RefFinder. *TFIIS*, *EF-1α*, and *CYP22* were the most suitable internal reference genes in the leaves of *L. rotata* from different regions, while *OBP*, *TFIIS*, and *CYP22* were the optimal reference genes in the roots of *L. rotata*. The reference genes identified here would be very useful for gene expression studies with different tissues in *L. rotata* from different habitats.

Keywords: *Lamiophlomis rotata*; reference genes; RT-qPCR; geNorm; NormFinder; Bestkeeper; RefFinder

Citation: Wang, L.; Qiao, F.; Geng, G.; Lu, Y. Evaluation of Candidate Reference Genes for Gene Expression Analysis in Wild *Lamiophlomis rotata*. *Genes* **2023**, *14*, 573. <https://doi.org/10.3390/genes14030573>

Academic Editors: Stefania Bortoluzzi, Piero Fariselli and Anelia D. Horvath

Received: 19 January 2023

Revised: 10 February 2023

Accepted: 22 February 2023

Published: 24 February 2023



Copyright: © 2023 by the authors. Licensee MDPI, Basel, Switzerland. This article is an open access article distributed under the terms and conditions of the Creative Commons Attribution (CC BY) license (<https://creativecommons.org/licenses/by/4.0/>).

1. Introduction

Real-time quantitative PCR (RT-qPCR) is an important technology for studying the gene expression pattern in the processes of plant growth and development and secondary metabolite synthesis [1–4]. It is characterized by high accuracy, strong specificity, and good repeatability [5]. In the process of DNA amplification, RT-qPCR can monitor the change in product content in real time and conduct a quantitative analysis through the change in fluorescence signal intensity, so it is often used for the study of gene expression [6]. However, the accuracy of the results of this technique is affected by various factors, such as the specificity of primers, the integrity of RNA, and the quality of cDNA. Among them, the stability of reference genes has the greatest impact [7]. The selection of appropriate internal reference genes for calibration can reduce the differences between samples and ensure the accuracy of RT-qPCR results [8]. Housekeeping genes have a stable expression and are not easily affected by environment, therefore, they are frequently used as internal reference genes for RT-qPCR analysis. Common housekeeping genes in plants include actin (*ACT*), 18S ribosomal RNA (*18S rRNA*), glyceraldehyde-3-phosphate dehydrogenase (*GAPDH*), elongation factor 1α (*EF-1α*), and polyubiquitin (*UBQ*) genes [9]. Given different species, tissues, and experimental conditions, the expression stability of internal reference genes will also be different [10]. For example, the stable expression of *GAPDH* in grape berries is the worst in wheat (*Triticum aestivum*) [11,12]. In the stems of

Psamochloa villosa, the *ACT* gene is the most suitable internal reference gene for gene expression research under drought conditions, while tubulin alpha chain (*TUA*) is the most stable and the best internal reference gene under cold conditions [13]. Therefore, screening internal reference genes in accordance with different species, tissues, and experimental conditions is necessary to ensure the accuracy of RT-qPCR results [14].

L. rotata (Benth.) Kudo (*L. rotata*) is a perennial wild herb of the Lamiaceae family, which is widely distributed in the Qinghai, Tibet, Sichuan, and Gansu provinces of China. It grows in meadow, grassland, and sand gravel regions at altitudes between 3100 and 5100 m. It is a commonly used Chinese herbal medicine of Tibetan, Naxi, Mongolian, and other ethnic groups in China [15,16]. The roots and leaves of *L. rotata* contain various active ingredients, such as iridoids, flavonoids, and phenylethanol glycosides [17–19]. In clinical practice, this herbal medicine is mainly used to treat traumatic bleeding, bruises, and other diseases [20–22]. The iridoid compounds, represented by gardenoside methyl ester and 8-O-acetyl gardenoside methyl ester, which have good hemostatic and procoagulant effects, are the main medicinal components of *L. rotata* [22]. Present research on *L. rotata* mainly focuses on the distribution of germplasm resources [15], the extraction, separation, and identification of chemical components [19], the pharmacological effects [23], and other aspects. However, research on the biosynthetic pathway of iridoid, flavonoid, and phenylethanol glycoside compounds in *L. rotata* has not been reported. It is very important to study the expression pattern of key genes in the biosynthetic pathway of secondary metabolism in wild *L. rotata*, and the research results could provide clues for the molecular mechanism of pharmaceutical ingredient accumulation in *L. rotata*. At present, no research has been conducted on the screening of the internal reference genes of *L. rotata*. Thus, screening the best internal reference gene in the RT-qPCR analysis of *L. rotata* is of great significance for the subsequent study and analysis of the gene expression pattern of *L. rotata*.

With the development of high-throughput sequencing technology, plant RNA-seq datasets can be obtained rapidly and comprehensively [24,25]. This technology is now widely used in transcriptome gene expression analysis [26], secondary metabolism studies of plants [27,28], disease resistance mechanisms [29], biocontrol [30,31], and so on. RNA-seq datasets can also be used to study the molecular function of specific genes and to screen for internal reference genes [32,33]. Therefore, in this study, based on the transcriptome data of leaves and roots in *L. rotata* from five regions (GL, XW, YS, ZD, and CD regions, Figure 1 and Table 1) through the Illumina high-throughput sequencing platform (Biomaker Technologies Company, Beijing, China), 15 candidate internal reference genes were finally screened based on the expression of FPKM >10 and difference ploidy < 2 [34], and included *actin 8* (*ACT8*), cyclophilin 22 (*CYP22*), cyclophilin 95 (*CYP95*), TIP 41-like protein (*TIP41*), translation elongation factor (*TFIIS*), *EF-1 α*, *actin 7* (*ACT7*), protein phosphatase 2A (*PP2A*), oxysterol-binding protein (*OBP*), tubulin β chain (*TUB*), cyclophilin23 (*CYP23*), ribochemical protein large subunit (*RPL*), anthranilate phosphoribosyltransferase (*TrpD*), acetylcholine deacetylase (*AO*), and α colloid NSF attachment protein (*SNAP*). The GeNorm, NormFinder, BestKeeper, and RefFinder algorithms were used to evaluate the expression stability of these candidate genes in the root and leaf tissues of *L. rotata* from different regions. Then, the selected best housekeeping gene could be used to analyze the expression pattern of the genes involved in the biosynthesis pathway of iridoid, flavonoid, and phenylethanol glycoside components of *L. rotata*. The objectives were to further verify the accuracy of the housekeeping gene and lay the foundation for the subsequent research on the functional verification of the genes involved in the biosynthesis pathway of these second metabolism components of *L. rotata*.

2. Materials and Methods

2.1. Experimental Materials

The wild materials of *L. rotata* used in this research were collected in Guoluo, Xiewu, Yushu, Zaduo, and Chengduo counties in Qinghai Province at different altitudes from 3750 m to 4270 m (Figure 1, Table 1). The root and leaf organs of *L. rotata* from the five areas were analyzed as experimental samples. The samples were placed in liquid nitrogen for rapid freezing and stored in a -80°C ultra-low-temperature freezer for the following experiments.



Figure 1. *L. rotata* in five different habitats. GL: Guoluo county in Qinghai province; XW: Xiewu county in Qinghai province; YS: Yushu county in Qinghai province; ZD: Zaduo county in Qinghai province; CD: Chengduo county in Qinghai province. Bar = 2 cm.

Table 1. The habitat and site of *L. rotata* from five regions.

Sample Name	Sampling Location	Altitude	East Longitude	North Latitude
GL	Guoluo county, Qinghai, China	3750 m	100°14'38"	34°29'10"
XW	Xiewu county, Qinghai, China	3860 m	97°21'3"	33°7'46"
YS	Yushu county, Qinghai, China	3880 m	97°1'23"	32°51'4"
ZD	Zaduo county, Qinghai, China	4208 m	95°10'48"	32°52'12"
CD	Chengduo county, Qinghai, China	4270 m	97°27'16"	33°18'2"

2.2. Total RNA Extraction and cDNA Synthesis

The total RNA was extracted from the roots and leaves of *L. rotata* from different regions by using a polysaccharide polyphenol plant RNA extraction kit (Nanjing Novozan Biotechnology Co., Ltd., Nanjing, China). The quality of RNA was assessed by 1% agarose gel electrophoresis. RNA was treated with DNase I (New England Biolabs) to remove DNA contamination as per the prescribed protocol.

The integrity of RNA was determined by observing the brightness of 18S rRNA and 28S rRNA bands through 1.2% agarose gel electrophoresis. The concentration of RNA was detected using a GeneQuant 100 ultraviolet spectrophotometer (Guangzhou Gangran Electromechanical Equipment Co., Ltd., Guangzhou, China), and its purity was determined with OD260/280. Each product used 1000 ng of RNA to synthesize the first strand of cDNA in accordance with the HiScript[®] II Q RT SuperMix for qPCR (+gDNA wiper) kit (Nanjing Novozan Biotechnology Co., Ltd., Nanjing, China), and the cDNA was stored in a -20°C low-temperature freezer for standby.

2.3. Screening of Candidate Internal Reference Genes and Designing of Primers

Based on the transcriptome data of the roots and leaves of *L. rotata* from different regions, 15 candidate internal reference genes, including *ACT8*, *CYP22*, *CYP95*, *TIP41*, *TFIIS*, *EF-1 α* , *ACT7*, *PP2A*, *OBP*, *TUB*, *CYP23*, *RPL*, *TrpD*, *AO*, and *SNAP*, were finally screened. In accordance with the nucleotide sequence of candidate internal reference genes, primers were designed using Primer 5.0 software (Table 2). The parameters were set as follows: GC content of 45–65%, primer length of 21–27 bp, primer annealing temperature of 60°C – 67°C , and amplification length of 80–200 bp. The primer was synthesized by Beijing Aoke Dingsheng Biotechnology Co., Ltd. (Beijing, China).

Table 2. Primer sequence information for reference genes in RT-qPCR analyses.

Gene Name	Gene Transcript Genbank No.	Primer Sequence	Product Length (bp)	Primer Efficiency
ACT8	OQ471970	F: ACTCACTTGCGGTCCAGTTATCC R: ATAACAGCTCCAGGGACTTCCAC	107	1.13
CYP22	OQ471972	F: CTTGACATCACCATCGGAAAC R: TTCCTGTATTGCGCTGTGCAGT	117	1.02
CYP95	OQ471971	F: GCAACGGTCTCTCCTCCAAGA R: CTCACAGGGCTTCGACTTGGT	86	0.90
TIP41	OQ471973	F: GGGAAGACTGCCAGGATCAAAT R: AGCCAGAAGCGCAAGAGAAGAT	175	1.07
TFIIS	OQ471974	F: GAGTTTGAGCCACGCTCGATT R: TCTTGCACCTCCCAAGTGA	163	1.02
EF-1 α	OQ471975	F: ACTGGGACTTCTCAGGCTGATTG R: CTGGCCTTGGAGTACTTTGGTGT	188	1.03
ACT7	OQ471976	F: CACCACCCGAAAGAAAGTACAGTG R: AGGACCCGATTCATCATACTCTCC	110	1.14
PP2A	OQ471977	F: GCTCATGTGTGCTCCCTCCT R: GCTGCCAGCCTCTTCACAAGT	155	1.05
OBP	OQ471978	F: GGAACCTCTTCTTGGCACAGA R: AACCAGACTTGGCGAGGTCAC	197	1.13
TUB	OQ471979	F: CAAACTCGCCGTGAACCTCAT R: CGTCCCACATTTGCTGGGTAA	134	1.14
CYP23	OQ471980	F: TGCGCCCTGTGCAATTCTATC R: AACTGTCTTTGGCGCGACACT	132	1.13
RPL	OQ471981	F: GAAACCCGCTGTCGTAAACC R: CTATCATCGCGCTTTCCTTCC	151	1.02
TrpD	OQ471982	F: CTGAGGCTGAGGCTTCTCTTGA R: CACCACCAGTCCCAACAATGTC	192	1.14
AO	OQ471983	F: GTCGCCTACAAGCCAAATAGGG R: GACGACATCCATGTGCATACCA	99	1.01
SNAP	OQ471984	F: GTATGAAGACGCTGCCGATTTG R: GCATTAGCTGCTTCATGCTTGC	141	1.14

2.4. RT-qPCR Analysis of the Candidate Internal Reference Genes

The original solution of cDNA extracted from the root and leaf organs of *L. rotata* from different regions and diluted 5 times was taken as the template. The QuantStudio™ 6 Flex System (Thermo Fisher Scientific, USA) was used to conduct RT-qPCR detection. The reaction system had the following components: 10 μ L of 2 \times ChamQ Universal SYBR qPCR Master Mix, 7.2 μ L of ddH₂O, 2 μ L of cDNA, and 0.4 μ L of upstream and downstream primers (10 μ M) each. The reaction conditions were as follows: predenaturation at 95 °C for 30 s, 95 °C for 10 s, and 60 °C for 30 s; 40 cycles. After amplification, the 60 °C–95 °C dissolution curve was analyzed to detect the specificity of the primers.

2.5. Determination of the Correlation Coefficient of Primer Pairs

The same amount of cDNA template stock solution of samples from different parts was mixed and diluted 5 times in turn. Five concentration gradients of the template stock solution were set, which were 5, 5⁻¹, 5⁻², 5⁻³, and 5⁻⁴. Each serial dilution was used separately in RT-qPCR to determine the threshold cycle (Ct) values of the candidate reference genes.

The primer specificity was verified by the presence of a single peak in the melt curve analysis during the RT-qPCR process. Three independent biological replicates and three technical repetitions were performed for each of the quantitative PCR experiments. The threshold cycle (Ct) was measured automatically, and correlation coefficients (R²), together with slope, were calculated from the standard curve based on a five-fold series

dilution of the cDNA templates. The corresponding RT-qPCR efficiencies (E) for each gene were determined from the given slope.

2.6. Stability Analysis of the Candidate Internal Reference Genes

GeNorm [35], NormFinder [36], BestKeeper [37], and RefFinder [38], four conventional software tools, were used for evaluating the stability of the candidate reference genes under various altitude habitats. The Ct values were changed to relative quantities (Q) with the formula $Q = 2^{-\Delta Ct}$, where ΔCt = each corresponding Ct – minimum Ct. Then, the Q-values were input into GeNorm and NormFinder to calculate stability values (SVs). GeNorm uses the average stability value (M value) to evaluate the expression stability, which involves the average pairwise variation between each reference gene and others. Genes with $M < 1.5$ are generally regarded as stable. Moreover, the GeNorm pairwise variation (V) values (V_n / V_{n+1}) were applied to define the most appropriate reference gene number. The recommended value is ≤ 0.15 when opting for an appropriate number of genes. The NormFinder software evaluates expression stability by calculating the SV (lower SV indicates higher stability) when applying reference genes for standardization. In BestKeeper, the most stable reference gene was evaluated by the coefficient of variance (CV) and standard deviation (SD), with lower CV and SD values meaning higher stability. The RefFinder tool (<http://blooge.cn/RefFinder/> accessed on 1–2 November 2022), integrating the outcomes of BestKeeper, Delta Ct, GeNorm, and NormFinder analysis, was applied to perform the most stable reference genes.

2.7. Validation of the Validity of the Candidate Reference Genes

When the selected reference gene was used as internal reference, the CT values of three genes encoding key enzymes (deoxyxylulose 5-phosphate synthase (DXS, EC 2.2.1.7), deoxyxylulose 5-phosphate reductoisomerase (DXR, EC1.1.1.267), and 4-hydroxy-3-methylbut2-en-1-yl diphosphate reductase (HDR, EC 1.17.1.2)) related to the biosynthesis of terpenoids were determined by RT-qPCR. The obtained Ct values were sorted out and analyzed quantitatively with $2^{-\Delta\Delta Ct}$ to verify the reliability of the candidate reference gene [39]. The primers of each target gene were designed by Primer Premier 5.0 software and shown in Table 3.

Table 3. Primer sequence information for target genes in *L. rotata*.

Gene Name	Gene Transcript Genbank No.	Primer Sequence (5'–3') (Forward/Reverse)	Amplicon Length (bp)
DXS	OQ471985	F: GAAGGGGAGAGGGTGGCTCTAT R: GAGCACCATCCAACGGCTTAC	136
HDR	OQ471986	F: CTTGCCGGAGACCAGAATATC R: GCCTTGGCGTTAAACTCAGAC	111
DXR	OQ471987	F: CGAGCAGAACTTGTCACATCG R: CTGCAAAGTAGCCGCGTAATC	84

3. Results

3.1. Primer Specificity and Correlation Coefficient of Primer Sets

Fifteen candidate reference genes were selected from the transcriptome of *L. rotata*. The specificity of each primer pair was assessed by agarose gel electrophoresis and melting curve analysis (Figure S1). For each candidate reference gene, the length of a single amplicon ranged from 86 bp to 197 bp (Table 2).

To check the efficiency of PCR amplification using these primers, the correlation coefficient (R^2) of each primer set was determined using the slopes of the curves obtained by serial dilutions. For this purpose, a dilution series of template samples containing cDNA and water in the ratio of 1:1, 1:5, 1:25, 1:125, and 1:625 was prepared, and RT-qPCR was performed (Figure 2). The plot of the Ct values versus the natural logarithm (ln) of

cDNA dilutions demonstrated a linear distribution for all primer sets (Figure 2). The calculation of R^2 indicated that all primer sets had R^2 values more than 0.95 (Figure 2). R^2 values between 0.80 and 1.00 are considered very good for any primer set. The amplification efficiency (E) of the primers was between 90% and 114% (Table 2). Based on the values of E and R^2 , we concluded that the primer specificity of each candidate reference gene was strong and thus can be used for screening candidate reference genes.

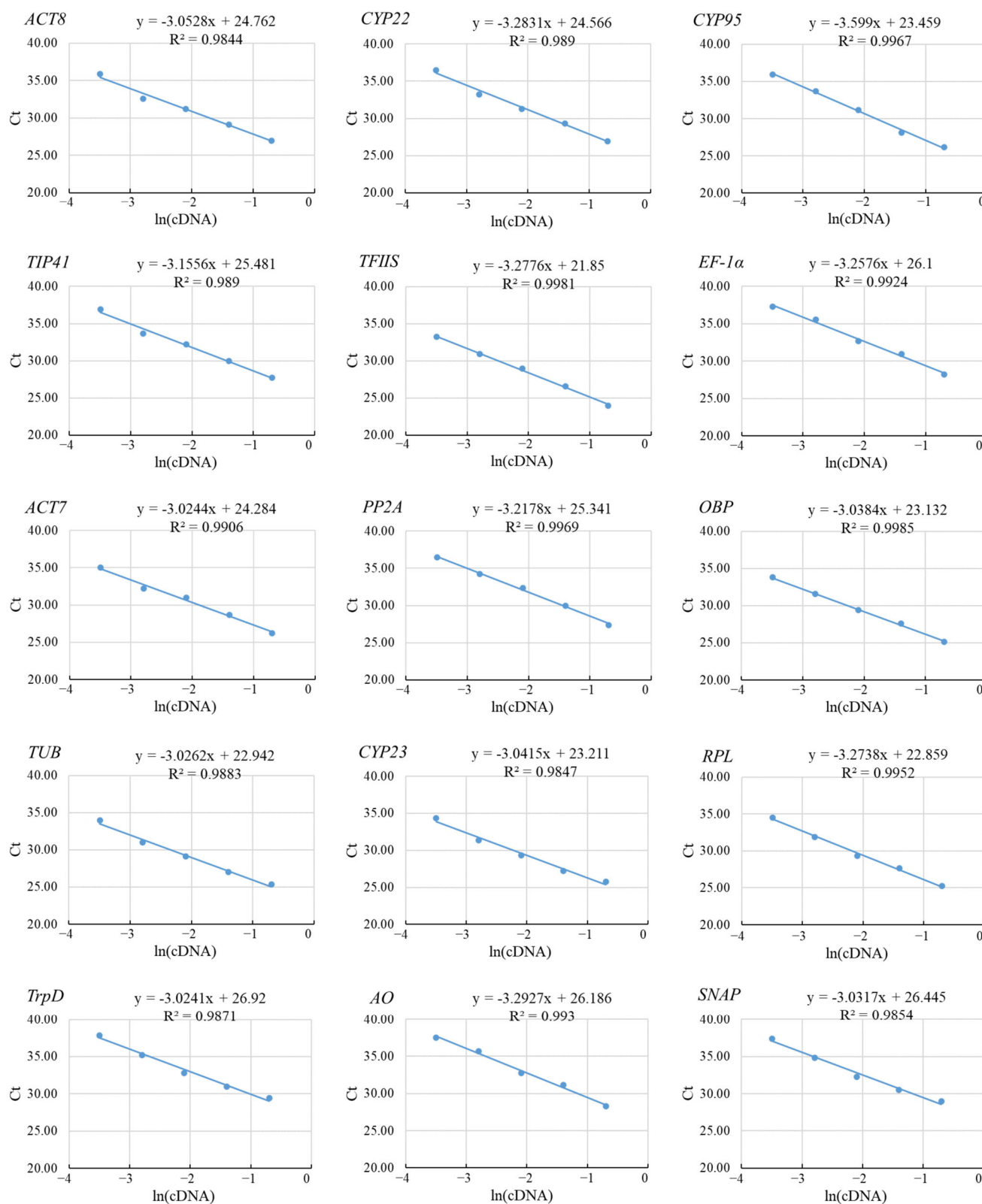


Figure 2. The correlation coefficient of each primer pair used for RT-qPCR. A graph of Ct value vs. the serial dilution factor of cDNA was drawn to determine the correlation coefficient (R^2). Its value for each reference gene has been mentioned within the respective graph.

3.2. Ct Values of the Candidate Reference Genes

Ct value can reflect the expression abundance of candidate internal reference genes in different samples. The Ct value of the 15 candidate internal reference genes in all samples was between 21 and 34. The Ct value across all the samples was shown in the form of a box and whisker plot (Figure 3). The median of the Ct values of the candidate reference genes ranged from 24.57 (for *EF-1 α*) to 32.33 (for *TrpD*). Lower Ct values implied higher expression levels and vice versa. The box and whisker plot indicated that *EF-1 α* and *ACT7* had the highest levels among all the candidate reference genes examined. With the median of the Ct value as the evaluation standard, *EF-1 α* had the highest expression level with a median of 24.57. The expression levels of *ACT7* and *OBP* were also relatively high, with median values of 25.69 and 26.75, respectively. Interestingly, genes with the lowest expression levels (*TrpD* and *SNAP*) showed smaller variability in their Ct values across different regions with median values of 32.23 and 32.11.

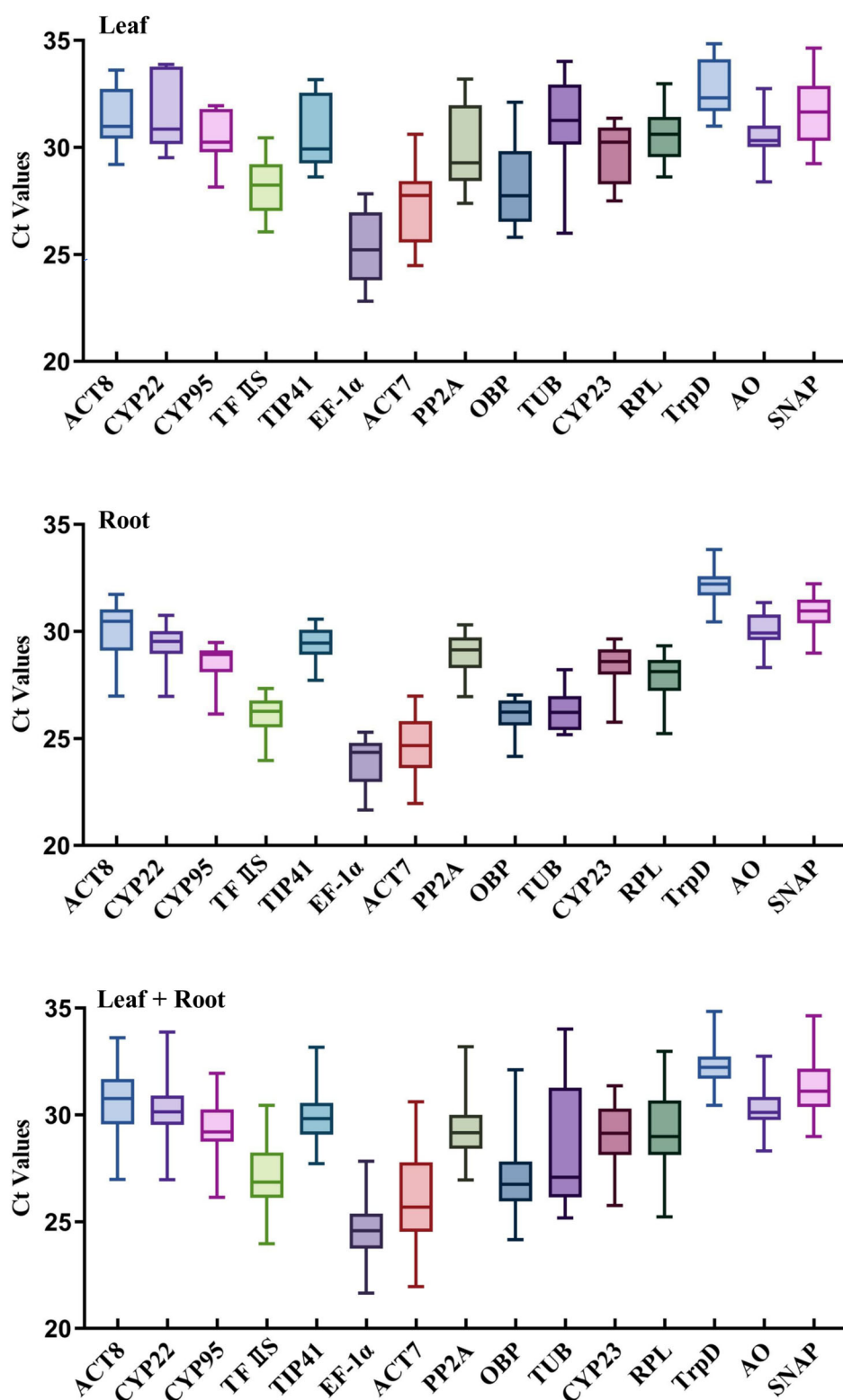


Figure 3. Gene expression levels of the candidate reference genes displayed as Ct values across leaf, root, and leaf + root samples of *L. rotata* from five habitats. The graph also shows the variation in Ct values for each reference gene. Whiskers across the box depict the highest and lowest values.

Similarly, Figure 3 shows that the upper and lower box lines and the maximum and minimum values of *CYP95* and *TFIIS* varied minimally in all samples. The expression of these two genes was preliminarily believed to be relatively stable in all samples. On the

contrary, the difference between the upper and lower quartiles and the maximum and minimum values of *TUB* was relatively large. The expression stability of this gene was speculated to be poor in all samples. Meanwhile, the difference of *RPL* and *ACT8* was small in leaves from different regions, which suggested that these two genes were relatively stable. In the root of *L. rotata* from different regions, the difference of *OBP* and *PP2A* was small, and these two genes were considered to be relatively stable.

3.3. Stability Analysis of the Candidate Reference Genes

To systematically evaluate the stability of the 15 candidate reference genes, this study used GeNorm, NormFinder, BestKeeper software, and the RefFinder online analysis tool to analyze the results of RT-qPCR.

3.3.1. GeNorm Analysis of the Stability of the Candidate Reference Genes

The stability of the 15 candidate reference genes was analyzed using GeNorm software. The stability was expressed by M value: the smaller the M value, the stronger the stability. The M value of the 15 candidate reference genes in each group was less than 1.5 (Figure 4), which indicated that the candidate reference genes had good stability. In all samples, the M value of *CYP22/TFIIS* was the smallest (0.54), whereas the M value of *TUB* was the largest (1.18). Accordingly, the expression stability of *CYP22/TFIIS* was the best in all samples, and it was the most suitable to be used as an internal reference gene. For the leaves with unique characteristics from different regions, the M values of the 15 candidate reference genes were ranked from largest to smallest as *TUB* > *AO* > *TrpD* > *OBP* > *ACT7* > *CYP23* > *SNAP* > *TIP41* > *CYP95* > *ACT8* > *RPL* > *PP2A* > *CYP22* > *TFIIS/EF-1 α* . However, in the roots of *L. rotata* from different regions, the M value of *TFIIS/OBP* was the smallest (0.25), which was greatly different from the stability evaluation results of all samples. The M value of *OBP* in all samples was speculated to be higher because of the poor expression stability in the leaves of *L. rotata* from different regions.

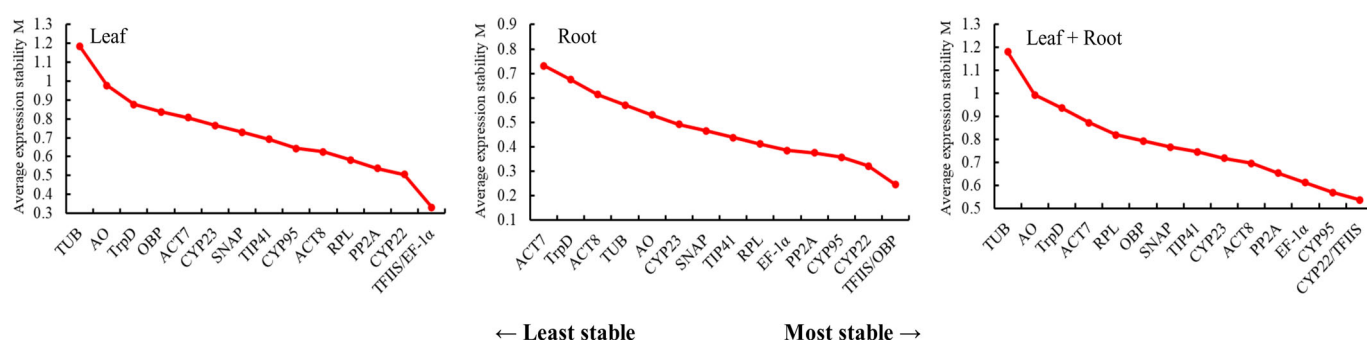


Figure 4. Average expression stability (M value) of fifteen candidate reference genes based on geNorm analyses. The most stably expressed reference genes have the lowest M values. M values were calculated for leaf, root, and leaf + root tissues of *L. rotata* from five habitats. Genes with M values lower than 1.5 may be used as candidate reference genes.

Through the GeNorm software, the 15 candidate reference genes were analyzed for the difference in candidate reference gene standardization factor pairs. The results (Figure 5) showed that $V2/V3$ was greater than 0.15 and $V3/V4$ was less than 0.15 in all samples and leaves from different regions. Therefore, three reference genes should be introduced in the RT-qPCR analysis of these two groups to make the results accurate and reliable. However, in the roots of *L. rotata* from different regions, $V2/V3$ (0.113) < 0.15, which indicated that the two internal reference genes can make the analysis accurate and reliable when RT-qPCR analysis was carried out in this group.

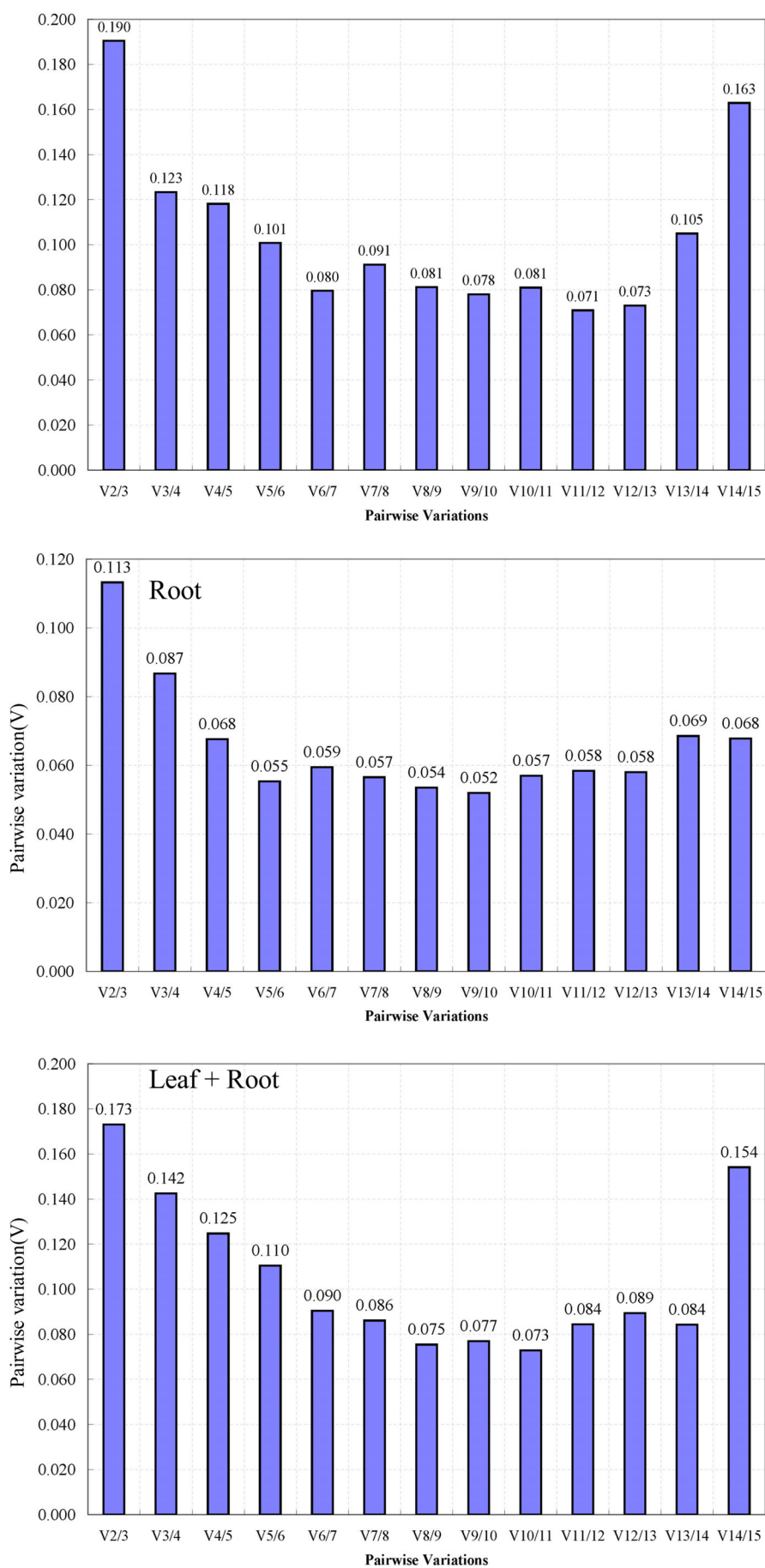


Figure 5. Determination of the optimal number of reference genes for each type of different habitat through geNorm analysis. Pairwise variation (V) was calculated by geNorm to determine the required number of reference genes for accurate normalization under different habitats. geNorm calculates pairwise variation (V_n / V_{n+1}) for the normalization factors NF_n and NF_{n+1} to determine ($V < 0.15$) the optimal number of reference genes.

3.3.2. NormFinder Analysis of the Stability of the Candidate Reference Genes

The stability of the 15 candidate reference genes was analyzed using NormFinder software. Similar to GeNorm, the lower the value is, the stronger the stability of genes is. In Figure 6, the stability sequencing results of different candidate reference genes in three different tissues were listed from left to right. In leaves from different regions, *TFIIS* had the best stability (0.22), whereas *TUB* had the worst stability (1.43). In the roots of *L. rotata* from different regions, the stability of *OBP* was the best (0.13), whereas the stability of *TrpD* was the worst (0.67). *CYP22* and *TFIIS* were stable in the top four in all experimental conditions and could be considered the best candidate reference genes. By contrast, *TUB* and *TrpD* had poor stability under all experimental conditions.

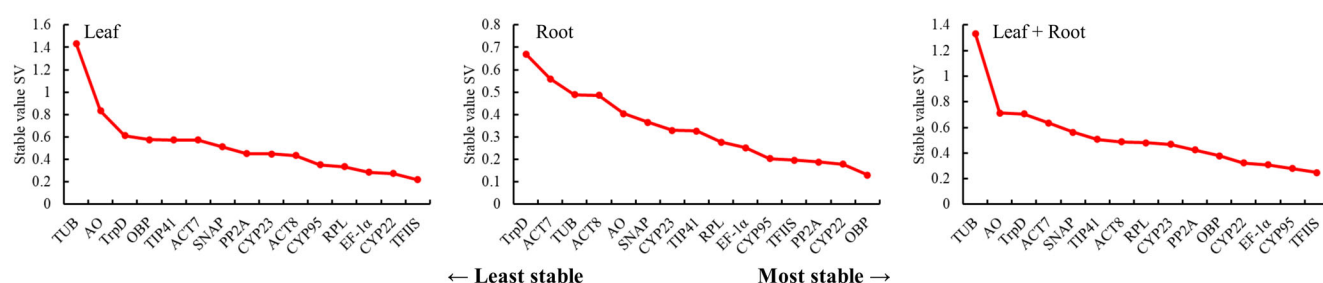


Figure 6. Expression stability values for 15 candidate reference genes calculated by NormFinder.

3.3.3. BestKeeper Analysis of the Stability of the Candidate Reference Genes

BestKeeper is an Excel-based algorithm, which directly uses the Ct value obtained from RT-qPCR analysis for further analysis. BestKeeper evaluates the stability of the candidate reference gene by calculating its CV and SD. Smaller CV and SD values represent better stability. From Table 4, in the leaves the stability of *OBP* (6.57 ± 1.86) was the worst, whereas that of *TrpD* (2.84 ± 0.92) and *CYP95* (3.51 ± 1.07) was the best. In the roots from different regions, the stability of *ACT7* (4.39 ± 1.08) was the worst, whereas that of *TrpD* (1.58 ± 0.51) and *AO* (1.65 ± 0.50) was the best. Under all experimental conditions, the stability of *TrpD* ranked first, and it was considered the most suitable reference gene.

Table 4. Ranking of candidate reference gene stability by BestKeeper analysis.

Reference Gene	Leaf + Root			Leaf			Root		
	CV Value	SD Value	Rank	CV Value	SD Value	Rank	CV Value	SD Value	Rank
<i>TrpD</i>	2.28	0.74	1	2.84	0.92	1	1.58	0.51	1
<i>AO</i>	2.79	0.85	2	4.09	1.27	6	1.65	0.50	2
<i>SNAP</i>	3.35	1.05	3	4.16	1.32	7	2.19	0.68	8
<i>CYP95</i>	3.39	1.00	4	3.51	1.07	2	2.39	0.68	10
<i>ACT8</i>	3.54	1.09	5	3.52	1.10	3	3.87	1.16	14
<i>CYP23</i>	3.58	1.04	6	3.86	1.15	5	2.90	0.82	12
<i>TIP41</i>	3.59	1.08	7	4.81	1.48	9	2.06	0.61	6
<i>PP2A</i>	3.73	1.10	8	5.40	1.62	11	1.88	0.55	3
<i>CYP22</i>	4.35	1.33	9	4.88	1.55	10	2.12	0.62	7
<i>EF-1α</i>	4.45	1.10	10	5.78	1.47	13	3.05	0.74	13
<i>TFIIS</i>	4.48	1.22	11	4.44	1.25	8	2.24	0.58	9
<i>RPL</i>	5.15	1.51	12	3.58	1.10	4	2.78	0.77	11

<i>OBP</i>	5.24	1.43	13	6.57	1.86	15	2.05	0.53	5
<i>ACT7</i>	6.46	1.68	14	5.51	1.51	12	4.39	1.08	15
<i>TUB</i>	9.35	2.68	15	6.02	1.86	14	2.01	0.53	4

3.3.4. RefFinder Analysis of the Stability of the Candidate Reference Genes

The RefFinder online analysis tool can take appropriate weight to comprehensively evaluate the analysis results of GeNorm, NormFinder, and BestKeeper, avoid the one-sidedness of single program analysis, and better analyze candidate internal reference genes [23]. In this study, 15 candidate internal reference genes were analyzed by RefFinder (Figure 7), and the results showed that the most suitable internal reference genes were *TFIIS*, *EF-1 α* , and *CYP22* in the leaves of *L. rotata* from different regions. The most suitable internal reference group in the roots of *L. rotata* from different regions included *OBP*, *TFIIS*, and *CYP22*. In all samples, the most suitable internal reference group was *TFIIS*, *CYP95*, and *CYP22* based on the analysis of RefFinder software.

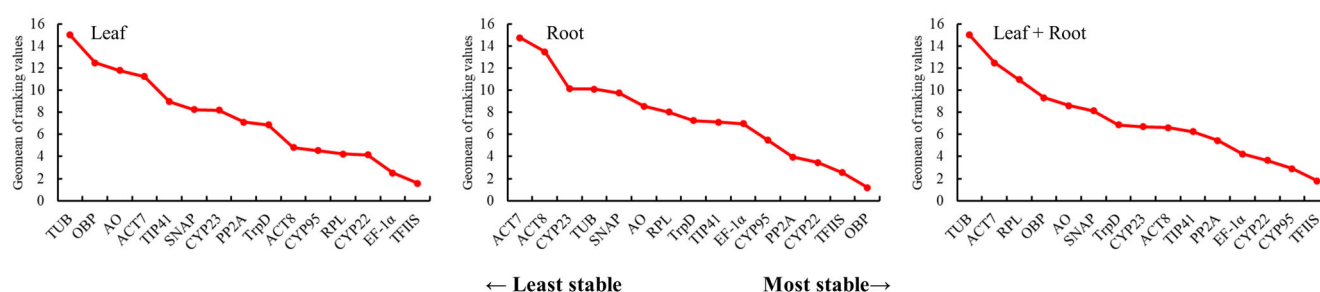


Figure 7. Ranking of candidate reference gene stability by RefFinder analysis.

3.4. Verification of the Stability of Internal Reference Genes

Three relatively stable internal reference genes (*TFIIS*, *EF-1 α* , and *CYP22*), and a poorly stable internal reference gene (*TIP41*) from the leaf, were used as the internal reference to study the expression of three genes (*DXR*, *HDR*, and *DXS*) related to the synthesis of iridoid compounds in the leaves of *L. rotata* from different regions. As shown in Figure 8, the three genes *DXR*, *HDR*, and *DXS* all showed the same expression change trend in the leaves of *L. rotata*.

Three stable internal reference genes (*TFIIS*, *OBP*, and *CYP22*) were also used to study the expression of the three genes *DXR*, *HDR*, and *DXS* in roots (Figure 8). Based on the two internal reference genes of *TFIIS* and *OBP*, the specific genes *DXR*, *HDR*, and *DXS* all showed the same expression change trend in the roots of *L. rotata* from five habitats.

Meanwhile, in the different tissues of *L. rotata* from different regions, different reference genes were screened as the most optimal internal reference genes. The three genes *TFIIS*, *EF-1 α* , and *CYP22* were found to be the three most stable reference genes in leaves (Table 4 and Figures 6–8). In roots, the three genes *TFIIS*, *OBP*, and *CYP22* were the most stable reference genes (Table 4 and Figures 6–8).

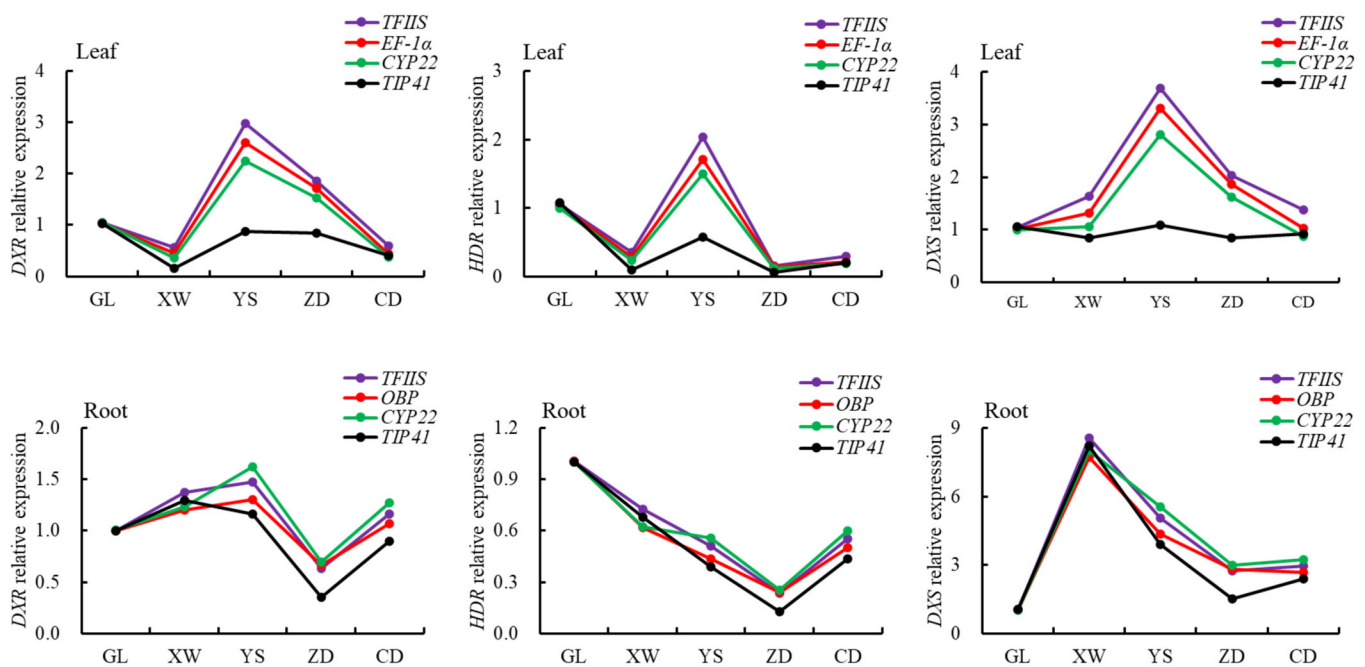


Figure 8. The relative expression of DXR, HDR, and DXS of *L. rotata* roots and leaves in different regions. *TFIIIS*, *EF-1α*, *CYP22*, *OBP*, and *TIP41* all were reference genes. DXR, HDR, and DXS all were target genes related to the biosynthetic pathway of iridoid compounds in *L. rotata*. The purple curve was based on the *TFIIIS* reference gene, the red curve was based on the *EF-1α* reference gene in leaves or *OBP* reference gene in roots, the green curve was based on the *CYP22* reference gene, and the black curve was based on the *TIP41* reference gene.

4. Discussion

RT-qPCR is a common technical means for studying gene expression patterns and analyzing gene functions and molecular mechanisms in molecular biology research. Appropriate reference genes are the prerequisite to ensure the accuracy of RT-qPCR data. In recent years, many scholars have analyzed the reference genes of different kinds of plants based on the RT-qPCR technology and found that the internal reference genes are not universal under the conditions of different plants, the same plant from different sources, and different parts of the same plant, and that the most suitable reference genes are different [40]. For example, in different tissues of *Isatis indigotica*, *CYP* was the most stable reference gene [41], but in all samples of *Lycoris aurea*, the stability of the *CYP* gene was poor [42]. The most stably expressed reference genes in the roots, stems, and leaves under high-light stress were *PSKS1*, *UBC2*, and *PSKS1*, respectively [43]. The *EF-1α* gene was identified as an unstable reference gene in response to herbicide stress in wild oat [44]. In all samples or different tissues of jute, the stability of *PP2A* gene expression was the best. On the contrary, in jute under drought stress, the stability of *PP2A* was poor, and the stability of the *ACT7* gene was the strongest [45]. The *ACT*, *RIB*, and *TUA* genes were the most stable reference genes expressed in different tissues of *Schima superba* [46]. Therefore, studying candidate reference genes from different sources and different parts is of great significance for improving the reliability of RT-qPCR results.

The identification of the optimal reference genes for specific conditions in a given species is imperative. Furthermore, our study revealed that the stability ranking of reference genes varied in certain circumstances due to the different algorithms used in the three analytical tools. In this study, the stability of candidate reference genes was evaluated for the first time for different regions and different parts of wild *L. rotata*. A total of 15 candidate reference genes were selected, and the expression stability of these 15 candidate reference genes in the roots and leaves of *L. rotata* from different regions was ana-

lyzed through GeNorm, NormFinder, and BestKeeper software. The results of the different software were generally consistent, but there were still differences. For example, based on the analysis of GeNorm, *TFIIS* and *EF-1α* were the best (Figure 4). The NormFinder analysis showed that the expression level of *TFIIS* was the most stable (Figure 6). Under the analysis of BestKeeper, *CYP95* and *TrpD* had the lowest degree of variation and the best stability. The differences were due to the fact that the algorithms of the three software are different; similar findings have been obtained in previous studies [46,47].

In order to screen the most suitable reference genes, the results obtained from the above three software programs were comprehensively analyzed using the online analysis tool RefFinder. The results showed that *TFIIS* and *EF-1α* were the most stable genes in the leaves of *L. rotata* in different regions based on the RefFinder method. The *TFIIS* gene is an important multifunctional protein, which can participate in gene translation regulation, cell signal pathway, and skeleton composition in organisms, and plays an important role in cell life activities. It is a common reference gene in plants at present [48]. *EF-1α* is a ubiquitous and conserved cytosolic protein among eukaryotic organisms and is responsible for catalyzing the binding of aminoacyl-transfer RNAs to ribosomes [49,50]. The expression of *OBP* and *TFIIS* was most stable in the roots of *L. rotata* in different regions based on the RefFinder method. The oxysterol-binding protein (*OBP*) is a storied protein in organelle biology and in sterol signaling and/or sterol transport functions [51]. Its major roles include acting as a membrane contact site tether, as well as a lipid antiporter [52]. Under Fe-deficient conditions, *OsOBP* and *OsLUG* were found to be the two most stable reference genes in any type of tissue taken in the study [53]. Among all the samples from different regions of *L. rotata*, *TFIIS* and *CYP95* were the most stable reference genes based on the RefFinder method. Plant cyclophilins (*CYPs*) are widely involved in a range of biological processes, including stress response, metabolic regulation, and growth and development [54,55]. *CYP* belongs to the immunophilin family and has peptidyl-prolyl *cis-trans* isomerase (PPIase) activity, which catalyzes the *cis-trans* isomerization process of proline residues. *CypA* demonstrated the most consistent expression irrespective of disease severity and emerged as the most suitable reference gene in COVID-19 and CAM [56].

In order to further verify the selected internal reference genes from the screen, we selected *DXR*, *DXS*, and *HDR* as the target genes. *DXR*, *DXS*, and *HDR* are key functional genes in the biosynthetic pathway of iridoid compounds and play roles in regulating the accumulation of downstream products and influencing the biosynthesis of iridoid compounds [57–59]. For example, the overexpression of the *DXR* gene induced by MeJ in *Tripterygium wilfordii* can increase the accumulation of triptophenolide [60]. Overexpression of the *DXS2* gene in the hairy root of *Salvia miltiorrhiza* will increase the content of tanshinone, while down-regulation of the *DXS2* gene will significantly reduce the content of tanshinone [61]. Overexpression of the *HDR* gene in *Nicotiana tabacum* will cause the expression of downstream genes related to terpene biosynthesis to be up-regulated, thus causing a significant increase in the accumulation of terpene compounds [62]. In this study, the expression levels of three target genes mentioned above were analyzed using the three most stable internal reference genes and one less stable internal reference gene. The results showed that the expression pattern of a same target gene (*DXR*, *DXS*, or *HDR*) was very similar although using the three most stable reference genes (*TFIIS*, *EF-1α*, or *CYP22* in leaves) (Figure 8), while the expression pattern of a same target gene (*DXR*, *DXS*, or *HDR*) changed more or less using a less internal reference gene (*TIP41*) (Figure 8). The validation results further illustrated the reliability of the RefFinder analysis results, and our study results also showed the importance of selecting the appropriate internal reference genes to ensure the reliability of RT-qPCR results.

5. Conclusions and Future Perspectives

The best genes for normalization of RT-qPCR in different tissues of *L. rotata* from different habitats are different. The three genes *TFIIS*, *EF-1α*, and *CYP22* are stable, viable

alternatives for data normalization in the leaves of *L. rotata*. Meanwhile, the genes *TFII*, *OBP*, and *CYP22* are the most stable reference genes in the roots of *L. rotata*. Our results reinforce the importance of the determination of the transcription stability of different candidate genes considering each experimental condition of interest. Our findings establish a solid foundation for further study of the gene regulatory network of *L. rotata* in response to different-altitude habitats. What is more, we can use the best reference genes screened from the leaves and roots of the wild *L. rotata* herb to analyze the expression changes of the genes related to the accumulation of the main medicinal compounds (iridoids, flavonoids, and phenylethanoids) of *L. rotata* and further explore the molecular regulation mechanism of the accumulation of the medicinal components of *L. rotata* at different altitudes.

Supplementary Materials: The following supporting information can be downloaded at <https://www.mdpi.com/article/10.3390/genes14030573/s1>, Figure S1.

Author Contributions: L.W.: contributed to the most experiments and analysis. F.Q.: designed the study, contributed to the experiments, and revised the manuscript. G.G.: field investigating and sampling, and formal analysis. Y.L.: field sampling and contributed to part of the experiments. All authors have read and agreed to the published version of the manuscript.

Funding: This study was supported by Science and Technology Department of Qinghai Province (2021-ZJ-729), Key Laboratory of Medicinal Animal and Plant Resources of Qinghai-Tibetan Plateau in Qinghai Province (2020-ZJ-Y04), Agricultural Resources and Environmental Protection Project of the Ministry of Agriculture and Rural Areas (125C0505).

Institutional Review Board Statement: Not applicable.

Informed Consent Statement: Not applicable.

Data Availability Statement: The data are available at <https://www.ncbi.nlm.nih.gov/Genbank/update.html>, GenBank accession numbers OQ471970; OQ471971; OQ471972; OQ471973; OQ471974; OQ471975; OQ471976; OQ471977; OQ471978; OQ471979; OQ471980; OQ471981; OQ471982; OQ471983; OQ471984; OQ471985; OQ471986; OQ471987.

Conflicts of Interest: The authors declare they have no conflict of interest.

Abbreviations: ACT7: actin 7, ACT 8: actin8, AO: acetylmethionine deacetylase, CYP22: cyclophilin 22, CYP95: cyclophilin 95, TIP 41: TIP 41-like protein, TFIIIS: transcription elongation factor, EF-1 α : elongation factor 1 α , PP2A: protein phosphatase 2A, OBP: oxysterol-binding protein, TUB: tubulin β chain, CYP 23: cyclophilin 23, RPL: ribosomal protein large subunit, TrpD: anthranilate phosphoribosyltransferase in tryptophan biosynthesis, SNAP: α -soluble NSF attachment protein, DXR: 1-deoxy-D-xylulose-5- phosphate reductoisomerase, DXS: 1-deoxy-D-xylulose- 5- phosphate synthase, HDR: 4-hydroxy-3-methylbut-2-enyl diphosphate reductase, GAPDH: glyceraldehyde -3- phosphate dehydrogenase, PP2Ac: catalytic subunit of protein phosphatase 2A, TUA: tubulin alfa chain, RIB: 60S ribosomal protein.

References

1. Li, Y.; Liang, X.; Zhou, X.; Wu, Z.; Yuan, L.; Wang, Y.; Li, Y. Selection of reference genes for qRT-PCR analysis in medicinal plant *Glycyrrhiza* under abiotic stresses and hormonal treatments. *Plants* **2020**, *9*, 1441. <https://doi.org/10.3390/plants9111441>.
2. Wang, W.; Hu, S.; Cao, Y.; Chen, R.; Wang, Z.; Cao, X. Selection and evaluation of reference genes for qRT-PCR of *Scutellaria baicalensis* Georgi under different experimental conditions. *Mol. Biol. Rep.* **2021**, *48*, 1115–1126. <https://doi.org/10.1007/s11033-021-06153-y>.
3. Lian, C.; Zhang, B.; Yang, J.; Lan, J.; Yang, H.; Guo, K.; Li, J.; Chen, S. Validation of suitable reference genes by various algorithms for gene expression analysis in *Isodon rubescens* under different abiotic stresses. *Sci. Rep.* **2022**, *12*, 19599. <https://doi.org/10.1038/s41598-022-22397-5>.
4. Wang, X.; Wu, Z.; Bao, W.; Hu, H.; Chen, M.; Chai, T.; Wang, H. Identification and evaluation of reference genes for quantitative real-time PCR analysis in *Polygonum cuspidatum* based on transcriptome data. *BMC Plant Biol.* **2019**, *19*, 498. <https://doi.org/10.1186/s12870-019-2108-0>.

5. Kou, X.Y.; Zhang, L.; Yang, S.Z.; Li, G.H.; Ye, J.L. Selection and validation of reference genes for quantitative RT-PCR analysis in peach fruit under different experimental conditions. *Sci. Hortic.* **2017**, *225*, 195–203. <https://doi.org/10.1016/j.sci-enta.2017.07.004>.
6. Bustin, S.A.; Benes, V.; Garson, J.A.; Hellemans, J.; Huggett, J.; Kubista, M.; Mueller, R.; Nolan, T.; Pfaffl, M.W.; Shipley, G.L.; et al. The MIQE guidelines: Minimum information for publication of quantitative real-time PCR experiments. *Clin. Chem.* **2009**, *55*, 611–622. <https://doi.org/10.1373/clinchem.2008.112797>.
7. Nolan, T.; Hands, R.E.; Bustin, S.A. Quantification of mRNA using real-time RT-PCR. *Nat. Protoc.* **2006**, *1*, 1559–1582. <https://doi.org/10.1038/nprot.2006.236>.
8. Xu, L.; Xu, H.; Cao, Y.; Yang, P.; Feng, Y.; Tang, Y.; Yuan, S.; Ming, J. Validation of reference genes for quantitative real-time PCR during bicolor Tepal development in Asiatic hybrid lilies (*Lilium* spp.). *Front. Plant Sci.* **2017**, *8*, 669. <https://doi.org/10.3389/fpls.2017.00669>.
9. Yuan, W.; Wan, H.J.; Yang, Y.J. Characterization and selection of reference genes for real-time quantitative RT-PCR of plants. *Chin. Bull. Bot.* **2012**, *47*, 427–436. <https://doi.org/10.3724/SP.J.1259.2012.00427>.
10. Sun, H.; Jiang, X.; Sun, M.; Cong, H.; Qiao, F. Evaluation of reference genes for normalizing RT-qPCR in leaves and suspension cells of *Cephalotaxus hainanensis* under various stimuli. *Plant Methods* **2019**, *15*, 31. <https://doi.org/10.1186/s13007-019-0415-y>.
11. Long, X.Y.; Wang, J.R.; Ouellet, T.; Rocheleau, H.; Wei, Y.M.; Pu, Z.E.; Jiang, Q.T.; Lan, X.J.; Zheng, Y.L. Genome-wide identification and evaluation of novel internal control genes for Q-PCR based transcript normalization in wheat. *Plant Mol. Biol.* **2010**, *74*, 307–311. <https://doi.org/10.1007/s11103-010-9666-8>.
12. Reid, K.E.; Olsson, N.; Schlosser, J.; Peng, F.; Lund, S.T. An optimized grapevine RNA isolation procedure and statistical determination of reference genes for real-time RT-PCR during berry development. *BMC Plant Biol.* **2006**, *6*, 27. <https://doi.org/10.1186/1471-2229-6-27>.
13. Liu, Y.P.; Zhang, Y.; Liu, F.; Liu, T.; Chen, J.Y.; Fu, G.; Zheng, C.Y.; Su, D.D.; Wang, Y.N.; Zhou, H.K. Establishment of reference (housekeeping) genes via quantitative real-time PCR for investigation of the genomic basis of abiotic stress resistance in *Psammochloa villosa* (Poaceae). *J. Plant Physiol.* **2022**, *268*, 153575. <https://doi.org/10.1016/j.jplph.2021.153575>.
14. Nicot, N.; Hausman, J.F.; Hoffmann, L.; Evers, D. Housekeeping gene selection for real-time RT-PCR normalization in potato during biotic and abiotic stress. *J. Exp. Bot.* **2005**, *56*, 2907–2914. <https://doi.org/10.1093/jxb/eri285>.
15. Li, Y.; Li, F.; Zheng, T.T.; Shi, L.; Zhang, Z.G.; Niu, T.M.; Wang, Q.Y.; Zhao, D.S.; Li, W.; Zhao, P. *Lamiophlomis herba*: A comprehensive overview of its chemical constituents, pharmacology, clinical applications, and quality control. *Biomed. Pharmacother.* **2021**, *144*, 112299. <https://doi.org/10.1016/j.biopha.2021.112299>.
16. Huang, X.J.; Wang, J.; Muhammad, A.; Tong, H.Y.; Wang, D.G.; Li, J.; Ihsan, A.; Yang, G.Z. Systems pharmacology-based dissection of mechanisms of Tibetan medicinal compound Ruteng as an effective treatment for collagen-induced arthritis rats. *J. Ethnopharmacol.* **2021**, *272*, 113953. <https://doi.org/10.1016/j.jep.2021.113953>.
17. Xia, M.; Zhang, Y.; Wu, H.; Zhang, Q.; Liu, Q.; Li, G.; Zhao, T.; Liu, X.; Zheng, S.; Qian, Z.; et al. Forsythoside B attenuates neuro-inflammation and neuronal apoptosis by inhibition of NF- κ B and p38-MAPK signaling pathways through activating Nrf2 post spinal cord injury. *Int. Immunopharmacol.* **2022**, *111*, 109120. <https://doi.org/10.1016/j.intimp.2022.109120>.
18. Ma, L.; Zhong, M.; Jiang, G.; Long, F.; Wu, W.; Jiang, Y. Elucidation of the active ingredients of *Lamiophlomis herba* against hemorrhage based on network pharmacology and tail snipping model in mice. *Pharmazie* **2020**, *8*, 381–384. <https://doi.org/10.1691/ph.2020.0507>.
19. La, M.; Zhang, F.; Gao, S.; Liu, X.; Wu, Z.; Sun, L.; Tao, X.; Chen, W. Constituent analysis and quality control of *Lamiophlomis rotata* by LC-TOF/MS and HPLC-UV. *J. Pharm. Biomed. Anal.* **2015**, *102*, 366–376. <https://doi.org/10.1016/j.jpba.2014.09.038>.
20. Zhao, X.; Jiang, S.; Dong, Q.; Dang, J.; Liu, Z.; Han, H.; Tao, Y.; Yue, H. Anti-rheumatoid arthritis effects of iridoid glucosides from *Lamiophlomis rotata* (Benth.) kudo on adjuvant-induced arthritis in rats by OPG/RANKL/NF- κ B signaling pathways. *J. Ethnopharmacol.* **2021**, *266*, 13402. <https://doi.org/10.1016/j.jep.2020.113402>.
21. Fan, P.C.; Ma, H.P.; Hao, Y.; He, X.R.; Sun, A.J.; Jiang, W.; Li, M.X.; Jing, L.L.; He, L.; Ma, J.; et al. A new anti-fibrinolytic hemostatic compound 8-O-acetyl shanzhiside methylester extracted from *Lamiophlomis rotata*. *J. Ethnopharmacol.* **2016**, *187*, 232–238. <https://doi.org/10.1016/j.jep.2016.04.016>.
22. Zhu, B.; Gong, N.; Fan, H.; Peng, C.S.; Ding, X.J.; Jiang, Y.; Wang, Y.X. *Lamiophlomis rotata*, an orally available Tibetan herbal painkiller, specifically reduces pain hypersensitivity states through the activation of spinal glucagon-like peptide-1 receptors. *Anesthesiology* **2014**, *121*, 835–851. <https://doi.org/10.1097/ALN.0000000000000320>.
23. Cui, Z.H.; Qin, S.S.; Zang, E.H.; Li, C.; Gao, L.; Li, Q.C.; Wang, Y.L.; Huang, X.Z.; Zhang, Z.Y.; Li, M.H. Traditional uses, phytochemistry, pharmacology and toxicology of *Lamiophlomis rotata* (Benth.) Kudo: A review. *RSC Adv.* **2020**, *10*, 11463–11474. <https://doi.org/10.1039/d0ra01050b>.
24. Guan, X.; Li, Z.; Zhou, Y.; Shao, W.; Zhang, D. Active learning for efficient analysis of high-throughput nanopore data. *Bioinformatics* **2023**, *39*, 764. <https://doi.org/10.1093/bioinformatics/btac764>.
25. Mursyidah, A.K.; Hafizzudin-Fedeli, M.; Nor Muhammad, N.A.; Latiff, A.; Firdaus-Raih, M.; Wan, K.L. Dissecting the biology of *Rafflesia* species: current progress and future directions made possible with high-throughput sequencing data. *Plant Cell Physiol.* **2023**, *00*, 1–10. <https://doi.org/10.1093/pcp/pcad004>.
26. Julca, I.; Tan, Q.W.; Mutwil, M. Toward kingdom-wide analyses of gene expression. *Trends Plant Sci.* **2023**, *28*, 235–249. <https://doi.org/10.1016/j.tplants.2022.09.007>.

27. Kapoor, B.; Kumar, A.; Kumar, P. Transcriptome repository of north-western himalayan endangered medicinal herbs: A paramount approach illuminating molecular perspective of phytoactive molecules and secondary metabolism. *Mol. Genet. Genom.* **2021**, *296*, 1177–1202. <https://doi.org/10.1007/s00438-021-01821-x>.
28. Tang, X.; Li, J.; Liu, L.; Jing, H.; Zuo, W.; Zeng, Y. Transcriptome analysis provides insights into *Potentilla bifurca* adaptation to high altitude. *Life* **2022**, *12*, 1337. <https://doi.org/10.3390/life12091337>.
29. Xiao, X.O.; Lin, W.; Feng, E.; Ou, X. Transcriptome and metabolome response of eggplant against *Ralstonia solanacearum* infection. *PeerJ* **2023**, *11*, 14658. <https://doi.org/10.7717/peerj.14658>.
30. Liang, N.; Charron, J.B.; Jabaji, S. Comparative transcriptome analysis reveals the biocontrol mechanism of *Bacillus velezensis* E68 against *Fusarium graminearum* DAOMC 180378, the causal agent of Fusarium head blight. *PLoS ONE* **2023**, *18*, 0277983. <https://doi.org/10.1371/journal.pone.0277983>.
31. Saberi Riseh, R.; Skorik, Y.A.; Thakur, V.K.; Moradi Pour, M.; Tamanadar, E.; Noghabi, S.S. Encapsulation of plant biocontrol bacteria with alginate as a main polymer material. *Int. J. Mol. Sci.* **2021**, *22*, 11165. <https://doi.org/10.3390/ijms22011165>.
32. Zhao, Z.; Zhang, Z.; Ding, Z.; Meng, H.; Shen, R.; Tang, H.; Liu, Y.G.; Chen, L. Public-transcriptome-database-assisted selection and validation of reliable reference genes for qRT-PCR in rice. *Sci. China Life Sci.* **2020**, *63*, 92–101. <https://doi.org/10.1007/s11427-019-1553-5>.
33. Bai, X.; Chen, T.; Wu, Y.; Tang, M.; Xu, Z.-F. Selection and validation of reference genes for qRT-PCR analysis in the oil-rich tuber crop tiger nut (*Cyperus esculentus*) based on transcriptome data. *Int. J. Mol. Sci.* **2021**, *22*, 2569. <https://doi.org/10.3390/ijms22052569>.
34. Dos Santos, K.C.G.; Desgagné-Penix, I.; Germain, H. Custom selected reference genes outperform pre-defined reference genes in transcriptomic analysis. *BMC Genom.* **2020**, *21*, 35. <https://doi.org/10.1186/s12864-019-6426-2>.
35. St-Pierre, J.; Grégoire, J.C.; Vaillancourt, C. A simple method to assess group difference in RT-qPCR reference gene selection using GeNorm: The case of the placental sex. *Sci. Rep.* **2017**, *7*, 16923. <https://doi.org/10.1038/s41598-017-16916-y>.
36. Andersen, C.L.; Jensen, J.L.; Ørntoft, T.F. Normalization of real-time quantitative reverse transcription-PCR data: A model-based variance estimation approach to identify genes suited for normalization, applied to bladder and colon cancer data sets. *Cancer Res.* **2004**, *64*, 5245–5250. <https://doi.org/10.1158/0008-5472.CAN-04-0496>.
37. Pfaffl, M.W.; Tichopad, A.; Prgomet, C.; Neuvians, T.P. Determination of stable housekeeping genes, differentially regulated target genes and sample integrity: BestKeeper—Excel-based tool using pair-wise correlations. *Biotechnol. Lett.* **2004**, *26*, 509–515. <https://doi.org/10.1023/b:bile.0000019559.84305.47>.
38. Xie, F.; Xiao, P.; Chen, D.; Xu, L.; Zhang, B. miRDeepFinder: A miRNA analysis tool for deep sequencing of plant small RNAs. *Plant Mol. Biol.* **2012**, *31*, 75–84. <https://doi.org/10.1007/s11103-012-9885-2>.
39. Pfaffl, M.W. A new mathematical model for relative quantification in real-time RT-PCR. *Nucleic Acids Res.* **2001**, *29*, e45. <https://doi.org/10.1093/nar/29.9.e45>.
40. Yao, J.; Zhu, G.; Liang, D.; He, B.; Wang, Y.; Cai, Y.; Zhang, Q. Reference gene selection for qPCR analysis in *Schima superba* under abiotic stress. *Genes* **2022**, *13*, 1887. <https://doi.org/10.3390/genes13101887>.
41. Qu, R.; Miao, Y.; Cui, Y.; Cao, Y.; Zhou, Y.; Tang, X.; Yang, J.; Wang, F. Selection of reference genes for the quantitative real-time PCR normalization of gene expression in *Isatis indigotica* fortune. *BMC Mol. Biol.* **2019**, *20*, 9. <https://doi.org/10.1186/s12867-019-0126-y>.
42. Ma, R.; Xu, S.; Zhao, Y.; Xia, B.; Wang, R. Selection and validation of appropriate reference genes for quantitative real-time PCR analysis of gene expression in *Lycoris aurea*. *Front. Plant. Sci.* **2016**, *7*, 536. <https://doi.org/10.3389/fpls.2016.00536>.
43. Yin, H.; Yin, D.; Zhang, M.; Gao, Z.; TuluHong, M.; Li, X.; Li, J.; Li, B.; Cui, G. Validation of appropriate reference genes for qRT-PCR normalization in oat (*Avena sativa* L.) under UV-B and high-light stresses. *Int. J. Mol. Sci.* **2022**, *23*, 11187. <https://doi.org/10.3390/ijms231911187>.
44. Akbarabadi, A.; Ismaili, A.; Kahrizi, D.; Nazarian Firouzabadi, F. Validation of expression stability of reference genes in response to herbicide stress in wild oat (*Avena ludoviciana*). *Cell Mol. Biol. (Noisy-le-grand)*, **2018**, *4*, 113–118.
45. Hossain, M.S.; Ahmed, R.; Haque, M.S.; Alam, M.M.; Islam, M.S. Identification and validation of reference genes for real-time quantitative RT-PCR analysis in jute. *BMC Mol. Biol.* **2019**, *20*, 13. <https://doi.org/10.1186/s12867-019-0130-2>.
46. Yang, Z.; Zhang, R.; Zhou, Z. Identification and validation of reference genes for gene expression analysis in *Schima superba*. *Genes* **2021**, *12*, 732. <https://doi.org/10.3390/genes12050732>.
47. Zhang, Z.; Li, C.; Zhang, J.; Chen, F.; Gong, Y.; Li, Y.; Su, Y.; Wei, Y.; Zhao, Y. Selection of the reference gene for expression normalization in *Papaver somniferum*, L. under abiotic stress and hormone treatment. *Genes* **2020**, *11*, 124. <https://doi.org/10.3390/genes11020124>.
48. Liu, C.; Wang, L.; Sun, Y.; Zhao, X.; Chen, T.; Su, X.; Guo, H.; Wang, Q.; Xi, X.; Ding, Y.; et al. Probe synthesis reveals eukaryotic translation elongation factor[1-Alpha]1 as the anti-pancreatic cancer target of BE-43547A. *Angew. Chem. Int. Ed. Engl.* **2022**, *61*, e202206953. <https://doi.org/10.1002/anie.202206953>.
49. Kristensen, R.; Torp, M.; Kosiak, B.; Holst-Jensen, A. Phylogeny and toxigenic potential is correlated in *Fusarium* species as revealed by partial translation elongation factor 1 alpha gene sequences. *Mycol. Res.* **2005**, *109*, 173–186. <https://doi.org/10.1017/s0953756204002114>.
50. Tatsuka, M.; Mitsui, H.; Wada, M.; Nagata, A.; Nojima, H.; Okayama, H. Elongation factor-1 α gene determines susceptibility to transformation. *Nature* **1992**, *359*, 333–336. <https://doi.org/10.1038/359333a0>.

51. Hammond, G.R.V.; Pacheco, J. Oxysterol binding protein: tether, transporter... and Flux Capacitor? *Trends Cell Biol.* **2019**, *29*, 531–533. <https://doi.org/10.1016/j.tcb.2019.04.004>.
52. Zhang, S.; Zhou, F.; Liu, Z.; Feng, X.; Li, Y.; Zhu, P. Inactivation of BoORP3a, an oxysterol-binding protein, causes a low wax phenotype in ornamental kale. *Hortic. Res.* **2022**, *9*, 219. <https://doi.org/10.1093/hr/uhac219>.
53. Soni, P.; Shivhare, R.; Kaur, A.; Bansal, S.; Sonah, H.; Deshmukh, R.; Giri, J.; Lata, C.; Ram, H. Reference gene identification for gene expression analysis in rice under different metal stress. *J. Biotechnol.* **2021**, *332*, 83–93. <https://doi.org/10.1016/j.jbiotec.2021.03.019>.
54. Qiao, Z.W.; Wang, D.R.; Wang, X.; You, C.X.; Wang, X.F. Genome-wide identification and stress response analysis of cyclophilin gene family in apple (*Malus × domestica*). *BMC Genom.* **2022**, *23*, 806. <https://doi.org/10.1186/s12864-022-08976-w>.
55. Chen, Q.; Chen, Q.-J.; Sun, G.-Q.; Zheng, K.; Yao, Z.-P.; Han, Y.-H.; Wang, L.-P.; Duan, Y.-J.; Yu, D.-Q.; Qu, Y.-Y. Genome-wide identification of cyclophilin gene family in cotton and expression analysis of the fibre development in *Gossypium barbadense*. *Int. J. Mol. Sci.* **2019**, *20*, 349. <https://doi.org/10.3390/ijms20020349>.
56. Kumar, S.; Ahmad, A.; Kushwaha, N.; Shokeen, N.; Negi, S.; Gautam, K.; Singh, A.; Tiwari, P.; Garg, R.; Agarwal, R.; et al. Selection of ideal reference genes for gene expression analysis in COVID-19 and Mucormycosis. *Microbiol. Spectr.* **2022**, *10*, e0165622. <https://doi.org/10.1128/spectrum.01656-22>.
57. Zhang, Y.; Zhao, Y.; Wang, J.; Hu, T.; Tong, Y.; Zhou, J.; Song, Y.; Gao, W.; Huang, L. Overexpression and RNA interference of *TwDXR* regulate the accumulation of terpenoid active ingredients in *Tripterygium wilfordii*. *Biotechnol. Lett.* **2018**, *40*, 419–425. <https://doi.org/10.1007/s10529-017-2484-1>.
58. Henriquez, M.A.; Soliman, A.; Li, G.; Hannoufa, A.; Ayele, B.T.; Daayf, F. Molecular cloning, functional characterization and expression of potato (*Solanum tuberosum*) 1-deoxy-d-xylulose 5-phosphate synthase 1 (*StDXS1*) in response to Phytophthora infestans. *Plant. Sci.* **2016**, *243*, 71–83. <https://doi.org/10.1016/j.plantsci.2015.12.001>.
59. Hao, G.; Shi, R.; Tao, R.; Fang, Q.; Jiang, X.; Ji, H.; Feng, L.; Huang, L. Cloning, molecular characterization and functional analysis of 1-hydroxy-2-methyl-2-(E)-butenyl-4-diphosphate reductase (*HDR*) gene for diterpenoid tanshinone biosynthesis in *Salvia miltiorrhiza* Bge. f. alba. *Plant Physiol. Biochem.* **2013**, *70*, 21–32. <https://doi.org/10.1016/j.plaphy.2013.05.010>.
60. Tong, Y.; Su, P.; Zhao, Y.; Zhang, M.; Wang, X.; Liu, Y.; Zhang, X.; Gao, W.; Huang, L. Molecular cloning and characterization of *DXS* and *DXR* genes in the terpenoid biosynthetic pathway of *Tripterygium wilfordii*. *Int. J. Mol. Sci.* **2015**, *16*, 25516–25535. <https://doi.org/10.3390/ijms161025516>.
61. Zhou, W.; Huang, F.; Li, S.; Wang, Y.; Zhou, C.; Shi, M.; Wang, J.; Chen, Y.; Wang, Y.; Wang, H.; et al. Molecular cloning and characterization of two 1-deoxy-D-xylulose-5-phosphate synthase genes involved in tanshinone biosynthesis in *Salvia miltiorrhiza*. *Mol. Breed.* **2016**, *36*, 124. <https://doi.org/10.1007/s11032-016-0550-3>.
62. Kim, Y.B.; Kim, S.M.; Sathasivam, R.; Kim, Y.K.; Park, S.U.; Kim, S.U. Overexpression of *Ginkgo biloba* Hydroxy-2-methyl-2-(E)-butenyl 4-diphosphate reductase 2 gene (*GbHDR2*) in *Nicotiana tabacum* cv. Xanthi. *3 Biotech.* **2021**, *11*, 337. <https://doi.org/10.1007/s13205-021-02887-5>.

Disclaimer/Publisher's Note: The statements, opinions and data contained in all publications are solely those of the individual author(s) and contributor(s) and not of MDPI and/or the editor(s). MDPI and/or the editor(s) disclaim responsibility for any injury to people or property resulting from any ideas, methods, instructions or products referred to in the content.